Understanding Ion Dynamics in Closoborate-Type Lithium-Ion Conductors on Different Time-Scales

Arunkumar Dorai[†,‡,*], *Sangryun Kim*[‡,¶,*], *Naoaki Kuwata*[†,§], *Junichi Kawamura*[†] , *Kazuaki Kisu*[‡] *and Shin-ichi Orimo*[‡,‖,*]

[†]Institute of Multidisciplinary Research for Advanced Materials (IMRAM), Tohoku University, Sendai-9808577, Miyagi, Japan

[‡]Institute of Materials Research (IMR), Tohoku University, Sendai-9808577, Miyagi, Japan

[§]National Institute of Materials Science, Tsukuba, Ibaraki, Japan

[‖]Advanced Institute for Materials Research (AIMR), Tohoku University, Sendai-9808577, Miyagi, Japan

[¶]Graduate School of Energy Convergence, Gwangju Institute of Science and Technology (GIST), 123 Cheomdangwagi-ro, Gwangju 61005, Republic of Korea

Corresponding Author

*dorai.arunkumar.c7@tohoku.ac.jp, sangryun@gist.ac.kr, shin-ichi.orimo.a6@tohoku.ac.jp

ABSTRACT The lithium-ion transport mechanism in $0.7Li(CB_9H_{10})–0.3Li(CB_{11}H_{12})$ complex hydride solid electrolyte was studied over a wide time-scale (ns–ms) by choosing appropriate techniques for assessing ionic motion on the desired time-scale using nuclear magnetic resonance (NMR) relaxation, AC impedance, and pulsed field gradient-NMR (PFG-NMR) measurements. The ^{7}Li NMR linewidth decreased with increasing temperature, and the spin-lattice relaxation time T_1 for the cation and anions showed a minimum near 303 K, indicating that the lithium ions and the anions were highly mobile. The activation energy estimated from the analysis of the NMR relaxation time matched well with the values estimated from the AC impedance and PFG-NMR. This confirms that the lithium-ion motion in $0.7Li(CB_9H_{10})–0.3Li(CB_{11}H_{12})$ is the same over a wide time-scale, suggesting steady Li-ion motion over a wide transport range. This understanding offers insights into strategies for designing complex hydride lithium superionic conductors.

.

TOC GRAPHICS

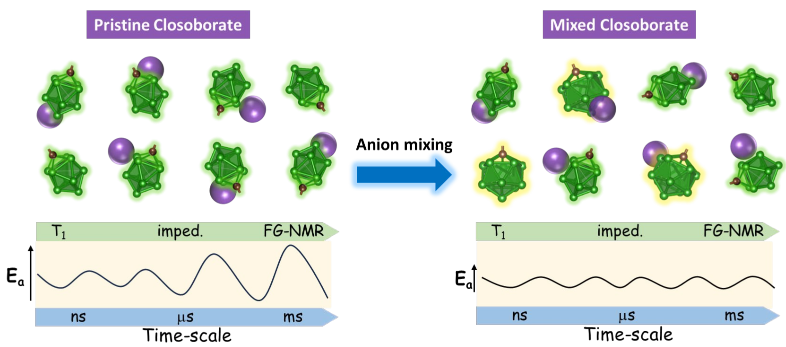

KEYWORDS Complex hydride, Lithium-ion conductors, ion dynamics, ^{7}Li NMR, NMR relaxation

Studies for developing all-solid-state lithium batteries have increased significantly as these batteries can prospectively address the drawbacks of current-generation lithium-ion batteries, including limited energy density, power density, and flammability. In the quest for suitable solid electrolytes for all-solid-state lithium batteries, three groups (oxide-[1,2], sulfide-,[3,4] and borohydride-based[5,6]) solid electrolytes have emerged as promising because of their high lithium-ion conductivity of ~10^{-3} S cm^{-1} at ambient temperature. Among these, complex hydride lithium-ion conductors are of great interest because of their high deformability and good chemical and electrochemical stability in lithium metal anodes.[7, 8]

Various closo-borohydride (borate) salts (MB_9H_{10}, $MB_{12}H_{12}$, MCB_9H_{10}, and $MCB_{11}H_{12}$ (M = Li, Na))[7] exhibit high ionic conductivity in the disordered high-temperature phase. Recently, we revealed that the partial replacement of CB_9H_{10} with the $CB_{11}H_{12}$ anion in $LiCB_9H_{10}$ stabilized the high-temperature disordered phase at lower temperatures, with extremely high lithium-ion conductivity at room temperature (~7 mS cm^{-1}).[8] The enhanced ionic conductivity was related to accelerated diffusive motion of the cation in the disordered phase formed by the partial replacement of $(CB_9H_{10})^-$ with $(CB_{11}H_{12})^-$. The cation mobility of closoborate-type compounds $MB_{12}H_{12}$ (M = Li, Na, K, Rb, Cs) is strongly associated with the reorientational motion of the anions (the so-called paddle-wheel mechanism).[9-12] The cation and anion motion in borohydrate-based systems ($LiBH_4$)[13] is decoupled, where reorientation of the anion occurs in picoseconds compared to cation conduction on the nanosecond time-scale. Despite attempts to study the ion dynamics in pristine borate compounds over a wide temperature range, such studies are hindered by phase transitions at high temperatures where the dynamics change rapidly. The high conductivity and structural stability of the $0.7Li(CB_9H_{10})$–$0.3Li(CB_{11}H_{12})$ borate system make it suitable for studying the cation and anion dynamics over a wide temperature range. Moreover, studying cation and anion dynamics on different time-scales can clarify the origin of the high conductivity.

Because cation and anion motion in solids occurs over a wide time-scale, interesting insight into the dynamics of the disordered phases can be obtained by examining the diffusion processes over different observation time-scales. Several research groups have attempted to study the relationship between the cation mobility and anion reorientational motion in MCB_nH_{n+1} closoborate systems (M = Li, Na, n = 9,11).[13-15] Various spectroscopic techniques such as quasi-elastic neutron scattering (QENS),[16] NMR spin-lattice relaxation,[9,17-19] PFG-NMR,[8,20] and AC impedance techniques have been used to investigate ion dynamics in different time domains (see Fig. 1). NMR spin-lattice relaxation measurements of the cation

(^{7}Li) and anion (^{1}H, ^{11}B) nuclei are effective for probing the ion dynamics in the short-range (ns–µs scale).[9,17-19] Similarly, PFG-NMR is effective for studying ion dynamics in Li-ion conducting solid electrolytes over longer time scales (ms–s).[8,20-23] AC impedance spectroscopic measurements bridge NMR-relaxation and PFG-NMR techniques, enabling analysis of the ion dynamics on the intermediate time-scale (µs–ms).[8,9,22,24] Therefore, by selecting appropriate measurement techniques, we can probe ion dynamics covering the best case for more than 10 decades[25, 26]. Apart from understanding the ion dynamics on different scales using the above-mentioned techniques, the Li ion diffusion coefficients calculated using each technique can be compared by using the Nernst-Einstein and Nernst-Smoluchowski relations, which relate the ionic conductivity (σ) and correlation time (τ) with the diffusion coefficient (D).

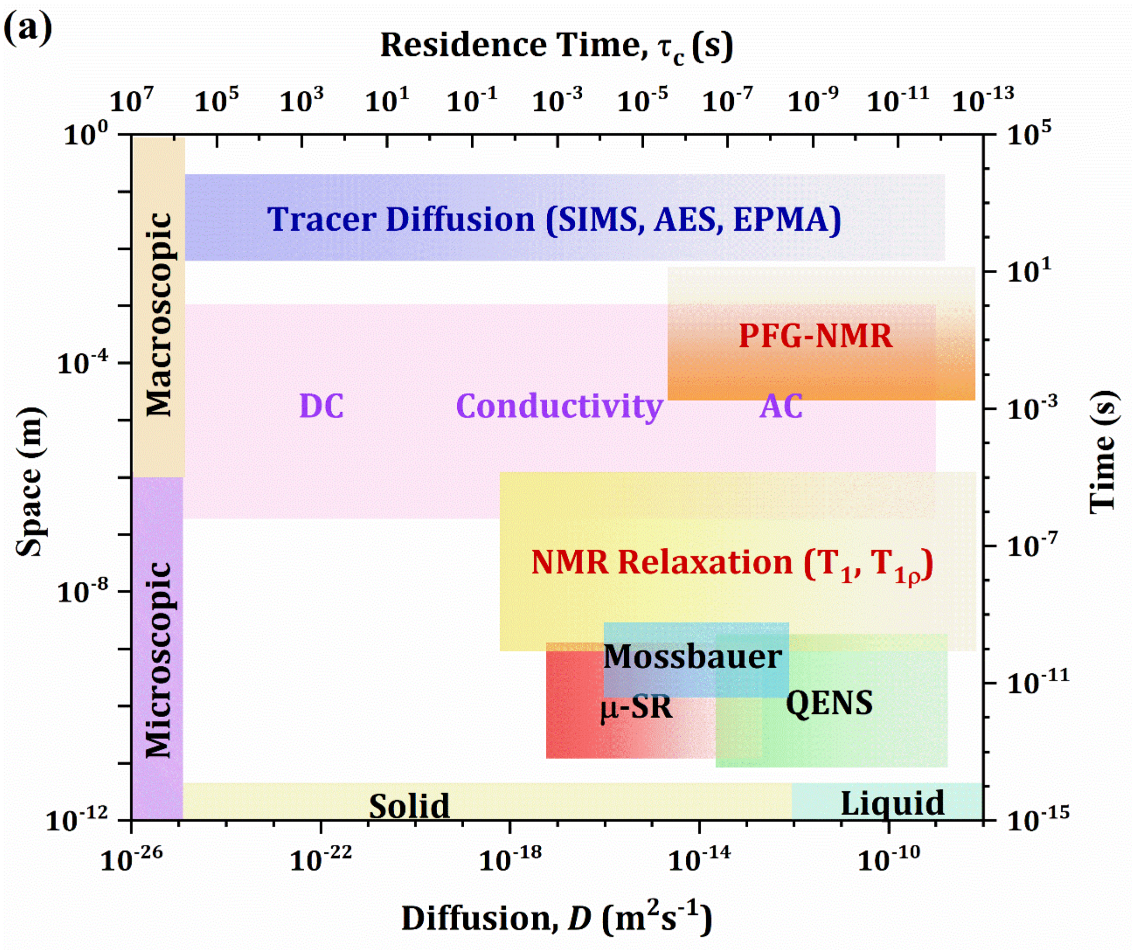

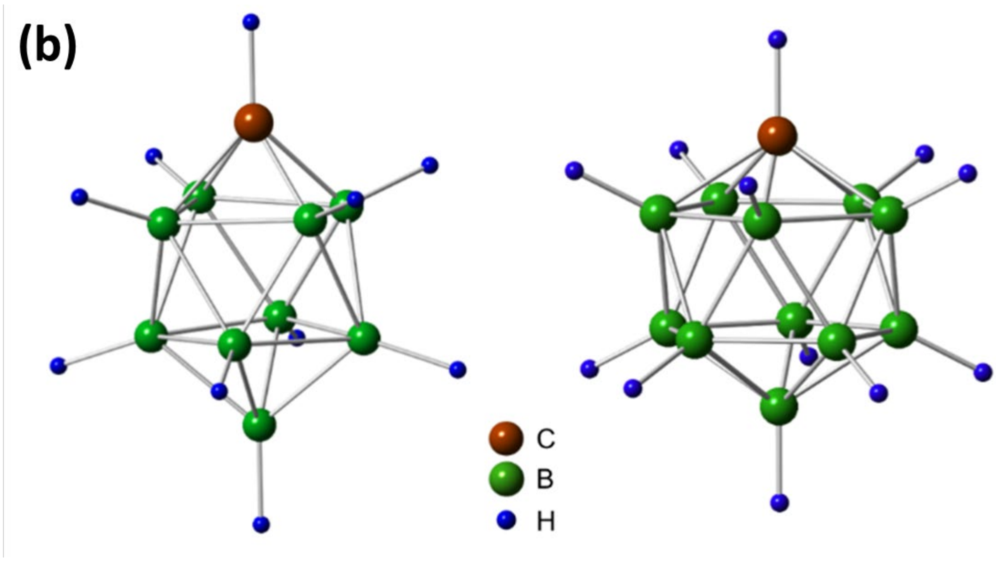

Figure 1. (a) Techniques for probing diffusion in solids with typical range of diffusivity and motional correlation time [25, 26], (b) structure of closoborate anions $(CB_9H_{10})^-$ and $(CB_{11}H_{12})^-$.

Using AC impedance and PFG-NMR spectroscopy (which falls in the µs–ms time scale), we previously established that disordered $0.7Li(CB_9H_{10})$–$0.3Li(CB_{11}H_{12})$ exhibits excellent lithium ion conducting properties.[8] Because the anion dynamics in disordered phases aid Li-ion conduction, studying the anion dynamics in these materials is significant. Moreover, the mixed closoborate sample $0.7Li(CB_9H_{10})$–$0.3Li(CB_{11}H_{12})$ did not show any structural transition with respect to temperature, which is typical for borohydride-based solid electrolytes, enabling us to the probe ion dynamics over a wide temperature range. As mentioned above, ion dynamics can be investigated on the nanosecond scale using NMR spin-lattice relaxation time measurements of cation (^7Li) and anion (^1H, ^{11}B) nuclei. In this study, we combine detailed ion dynamic analyses in different time-scales using NMR relaxation, AC impedance, and PFG-NMR techniques to investigate the ion transport properties of lithium ions in $0.7Li(CB_9H_{10})$–$0.3Li(CB_{11}H_{12})$, a closoborate solid electrolyte. The results indicate that the lithium-ion diffusion process shows less time-dependence within the measured time-scale because of the dynamically flat energy landscape caused by the disorder created by the partial mixing of anions.

General information regarding the static and dynamic properties of solids can be obtained using NMR linewidth and relaxation time (i.e., the times that characterize the flow of energy between the spin system and other systems) measurements.[27] In the case of lithium-ion-conducting solids with a closoborate structure, the anion plays an active role in the conduction mechanism. Therefore, ^7Li, ^1H, and ^{11}B NMR measurements were used to probe the bulk mobilities of the cations and anions in $0.7Li(CB_9H_{10})–0.3Li(CB_{11}H_{12})$. Moreover, the temperature-dependence of the static ^7Li NMR spectra is a valuable tool for obtaining insight into Li dynamics in crystalline solids.

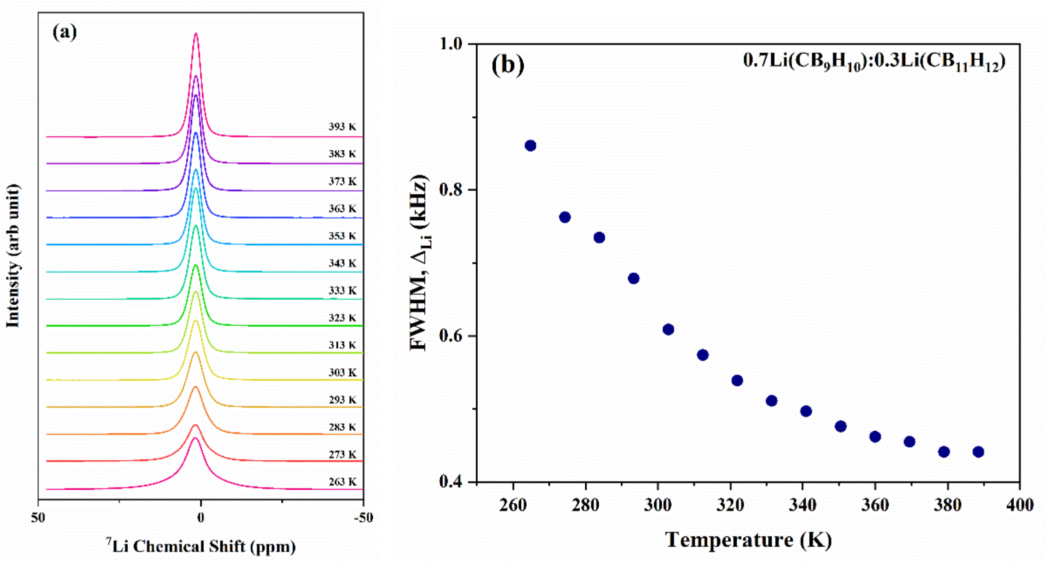

Figure 2. Temperature-dependence of (a) ^7Li NMR spectra and (b) ^7Li NMR linewidth for $0.7Li(CB_9H_{10})–0.3Li(CB_{11}H_{12})$.

The temperature-dependent ^7Li NMR spectra of $0.7Li(CB_9H_{10})–0.3Li(CB_{11}H_{12})$ (Fig. 2a) demonstrate that at low temperatures, the ^7Li NMR spectra are marginally broad, indicating faster ionic motion and narrows with respect to temperature. The temperature dependence of full width at half maxima (FWHM) Δ_{Li} of the ^7Li NMR spectra for $0.7Li(CB_9H_{10})–0.3Li(CB_{11}H_{12})$ is shown in Fig. 2b together with the Δ_{Li} of parent compounds $Li(CB_9H_{10})$[20] and $Li(CB_{11}H_{12})$[17]. The broad spectra at low temperatures for the parent compounds arises from the very strong dipolar interactions between the Li ions with very low mobility. With an increase in temperature due to the increase in the mobility of the Li ions, the NMR spectra became narrow (motional narrowing) due to weakening of the dipolar interaction.[28] Also at very high temperatures the FWHM shows a plateau indicating that the fast translational motion of the Li ions which is called as the rapid motion limit regime. For the mixed closoborate $0.7Li(CB_9H_{10})–0.3Li(CB_{11}H_{12})$, $\Delta_{Li} < 1$ kHz within the measured temperature range and is nearly equal to Δ_{Li} of $LiCB_9H_{10}$[7,20] and $LiCB_{11}H_{12}$[17] in the disordered phase. Also it is clear that, the onset of motional narrowing (T_{MN}) occurred at temperatures <260 K for $0.7Li(CB_9H_{10})–0.3Li(CB_{11}H_{12})$. Compared to the parent compounds the extreme narrowing regime where $\Delta_{Li} < 1$ kHz is observed at much lower temperatures in $0.7Li(CB_9H_{10})–$

$0.3Li(CB_{11}H_{12})$, indicating that the ^{7}Li-^{7}Li dipolar interactions to be completely averaged out due to the fast lithium motion. These results confirm that long-range fast translational motion of the Li ions to occur even at lower temperatures.[24]

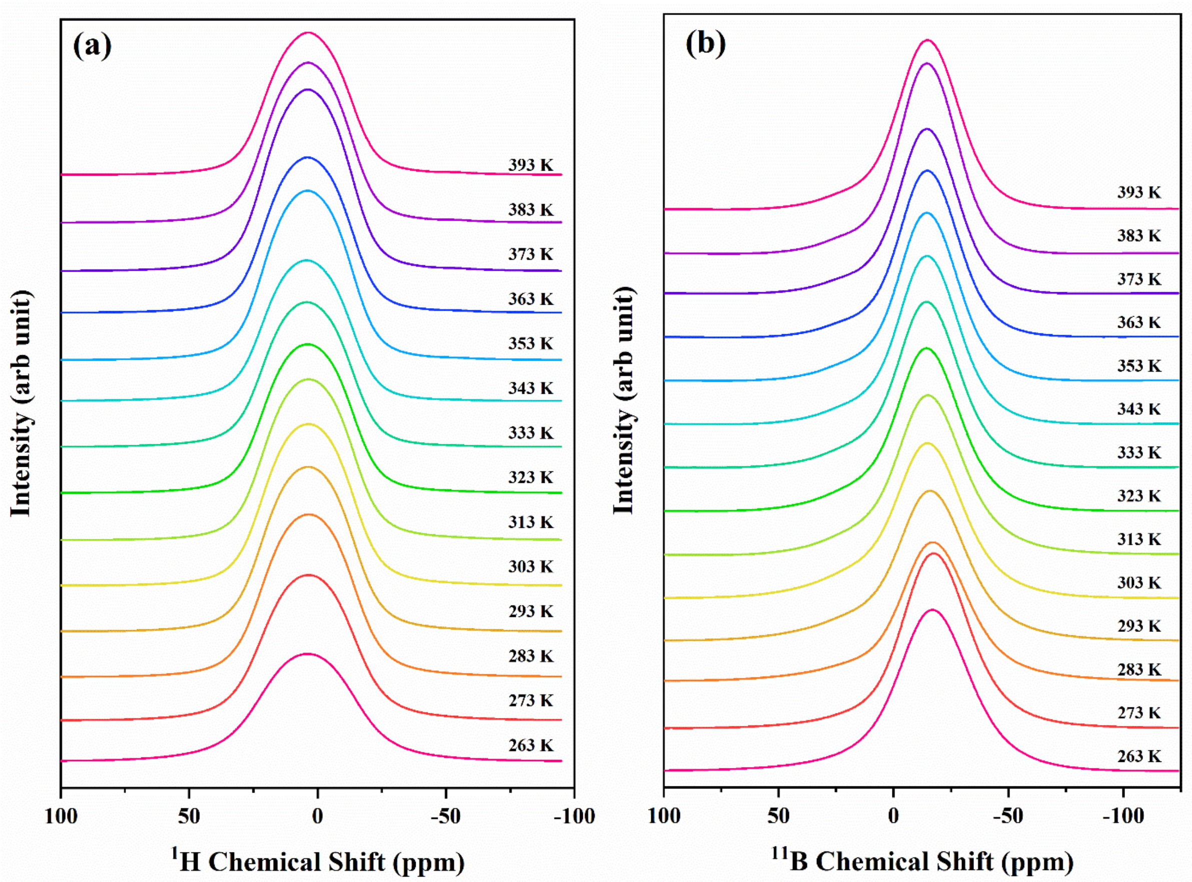

Figure 3. Temperature-dependence of (a) ^{1}H and (b) ^{11}B NMR spectra for $0.7Li(CB_9H_{10})$–$0.3Li(CB_{11}H_{12})$.

Figure 3(a, b) shows the temperature-dependence of the ^{1}H and ^{11}B NMR spectra of $0.7Li(CB_9H_{10})$–$0.3Li(CB_{11}H_{12})$. The slight temperature-dependent change in the linewidth indicates partial averaging of the dipole-dipole interactions of the ^{1}H spins due to the reorientational motion of the anion (Fig. 3a). Earlier studies on closoborate anions, such as CB_9H_{10} and $CB_{11}H_{12}$, reported that the ^{1}H NMR rigid lattice linewidth was approximately 50 kHz based on structural data and the linewidth narrowing to occur in two stages with respect to temperature. In the first stage, the narrowing of the ^{1}H NMR peaks was attributed to H motion, with jump rates exceeding 10^5 s^{-1}. In the second stage, a small step-like behavior was observed, which is attributed to weak cation-anion dipole-dipole interactions due to the translational diffusion of the cations.[16,17] At high temperatures, the ^{1}H NMR FWHM for CB_9H_{10} and $CB_{11}H_{12}$ reached a plateau value at approximately 10 kHz, indicating the involvement of H atoms in localized motion (anion reorientation). Moreover, non-zeroing of the FWHM indicates that the intramolecular interactions within each closoborate anion group to be completely averaged out by the reorientation motion, whereas the intermolecular interactions between different closoborate anion groups were not averaged out. Herein, the estimated NMR linewidth was ~12 kHz at 263 K, but decreased to 11 kHz at higher temperatures, and thereafter remained unchanged (Fig. S1). The linewidth of ~10 kHz for the present sample indicates that the intramolecular interactions within the anion were averaged out, even at the lowest measured temperature. The non-zeroing of the ^{1}H NMR linewidths is due to the non-averaging of the dipole-dipole interactions between the different anion molecules (intermolecular). The contribution from the ^{7}Li-^{1}H dipole-dipole interaction due to the translational motion of Li ions may also be present at high temperatures. The behavior of the ^{11}B NMR spectra and linewidth was similar to that of the ^{1}H NMR data.

Comparison of the ^{7}Li and ^{1}H NMR FWHM near 300 K indicates that the ^{7}Li NMR linewidth (Δ_{Li} = 0.6 kHz) for 0.7Li(CB_9H_{10})–0.3Li($CB_{11}H_{12}$) was much smaller than the ^{1}H NMR linewidth (Δ_{H} = 10 kHz). The smaller NMR linewidth for the Li cations arises because the dipole-dipole interactions are averaged out owing to the fast translational diffusion, whereas the larger linewidth for the anions is due to the partial averaging of the dipole-dipole interactions in the anions.

The microscopic Li-ion diffusion process in 0.7Li(CB_9H_{10})–0.3Li($CB_{11}H_{12}$) was investigated by analyzing the ^{7}Li spin-lattice relaxation rate over a broad temperature range. The spin-lattice relaxation rate (R_1), of nuclear spins can sensitively probe a motion with a rate of the order of the Larmor frequency (ω_0). Because ω_0 is in the MHz range, the R_1 measurements are sensitive to motional processes covering the nano–microsecond scale. At sufficiently high temperatures, the characteristic relaxation rate is mainly influenced by the diffusive motion of the ion itself or that sensed by the ion if neighboring species are involved in rapid motional processes. In the case of the diffusion-induced relaxation process, the plot of R_1 versus the inverse temperature ($1/T$) passes through a maximum. R_1 reaches its maximum when the mean correlation time is almost equal to the Larmor frequency. The temperature-dependent ^{7}Li spin-lattice relaxation rates (R_1) for the cations and anions in 0.7Li(CB_9H_{10})–0.3Li($CB_{11}H_{12}$) are shown in Fig. 4a. R_1^{Li}(T), R_1^{H}(T), and R_1^{B}(T) exhibit peak maxima around ambient temperature, which indicates that the cationic jump rate and anionic reorientational rate are of the order of ~10^9 s^{-1}.

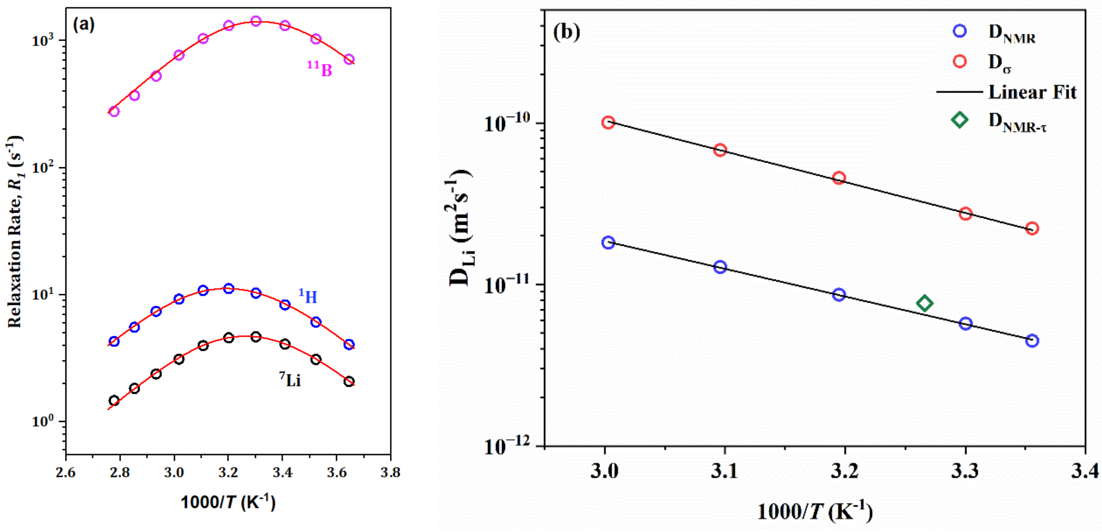

Figure 4. (a) Temperature-dependence of ^{7}Li, ^{1}H, and ^{11}B T_1 relaxation rate and (b) comparison of diffusion coefficient estimated using different techniques for 0.7Li(CB_9H_{10})–0.3Li($CB_{11}H_{12}$). Fig. 4b redrawn from Ref. 8.

The lithium-ion dynamics on the nanosecond scale were investigated using the ^{7}Li spin-lattice relaxation rate for 0.7Li(CB_9H_{10})–0.3Li($CB_{11}H_{12}$) (Fig. 4a). The temperature-dependence of the lithium spin-lattice relaxation rate $R_1^{Li}(T)$ shows a maximum at approximately 300 K, indicating that the cationic jump rate is nearly equal to the Larmor resonance frequency around this temperature. The appearance of the R_1 maximum at ambient temperature provides strong evidence of the fast motion of the Li^+ cation in this sample. Moreover, the relaxation rate maximum R_1^{Li} is observed at 5 s^{-1}, which is lesser than the ^{23}Na (R_{Na} ~ 300 s^{-1}) relaxation rate maxima observed for $NaCB_{11}H_{12}$[17] where quadrupolar interaction is the dominant contribution indicating that the dipole-dipole interactions of ^{7}Li to give significant contribution. Similar to $LiCB_{11}H_{12}$[17] system, the ^{7}Li NMR spin-lattice relaxation was confirmed to be dominated by dipolar contributions due to the translational motion (Li^+ diffusive jumps) of the Li ions. From the temperature dependent ^{7}Li NMR linewidth results, ^{7}Li-^{7}Li dipolar interactions is observed to be completely averaged out is negligible to contribute to the ^{7}Li relaxation mechanism. Therefore, for the present analysis we have considered the ^{7}Li-^{1}H dipolar interactions[17] to fit the ^{7}Li spin lattice relaxation rate R_1^{Li} using the Bloembergen Purcell Pound (BPP)[29] equation:

$$R_1^{Li} = \frac{\Delta M_{LiH}}{2}\left[\frac{\tau_c}{1+(\omega_H-\omega_{Li})^2\tau_c^2}+\frac{3\tau_c}{1+\omega_H^2\tau_c^2}+\frac{6\tau_c}{1+(\omega_H+\omega_{Li})^2\tau_c^2}\right]$$

where ΔM_{LiH} is the magnetic second moment. The correlation rate τ_C is defined by the Arrhenius expression ($\tau_C = \tau_0\, exp(-E_a\, /\, (k_B T))$). For fitting purposes, the magnetic second moment was a free parameter and the best fit obtained using the above expression is shown by the red solid line in Fig. 4a. The corresponding fitting parameters are E_a = 0.35 ± 0.01 eV, τ_0 = 6.70 ± 0.05 × 10^{-16} s, and ΔM_{LiH} = 4.15 ± 0.1 × 10^9 s^{-2}. The jump distance estimated from the diffusion coefficient and correlation rate from the spin-lattice relaxation data is 1.36 ± 0.1 Å (diffusion coefficient data for $0.7Li(CB_9H_{10})$–$0.3Li(CB_{11}H_{12})$ [8] was used). Moreover, the ^7Li relaxation rate showed a symmetric peak, indicative of ionic motion that remained unchanged within the evaluated temperature range.[30,31]

Similar to the ^7Li relaxation rate, peak maxima were observed for the ^1H and ^{11}B nuclei and for the relaxation rate with respect to temperature. The appearance of the R_1 maxima for ^1H at the same temperature as in the ^7Li relaxation rate spectrum indicates that the relaxation is strongly correlated with the motion of the Li ions. The appearance of an R_1 maximum in the anion spin-lattice relaxation rate spectra due to cation diffusion is common in several Li-conducting solid electrolytes.[32,33] Various interactions contribute to the relaxation process, including intramolecular (^1H-^1H, ^1H-^{11}B) and intermolecular (^7Li-^1H) interactions. From the temperature-dependence of the ^1H NMR linewidth, because the FWHM was ~12 kHz even at low temperatures, it is concluded that the intramolecular dipole-dipole interactions in the anion were averaged out completely, whereas the intermolecular dipole-dipole interactions persisted. Therefore, it is proposed that the intermolecular ^1H-^1H homonuclear and ^1H-^{11}B heteronuclear dipole-dipole interactions contribute to the relaxation of the ^1H nucleus, which can be expressed by the following equation:

$$R_1^H = \frac{2\Delta M_{HH}}{3}\left[\frac{\tau_c}{1+\omega_H^2\tau_c^2} + \frac{4\tau_c}{1+4\omega_H^2\tau_c^2}\right] + \frac{\Delta M_{HB}}{2}\left[\frac{\tau_c}{1+(\omega_H-\omega_B)^2\tau_c^2} + \frac{3\tau_c}{1+\omega_H^2\tau_c^2} + \frac{6\tau_c}{1+(\omega_H+\omega_B)^2\tau_c^2}\right]$$

where ω_H and ω_B are the resonance frequencies of ^1H and ^{11}B, respectively. ΔM_{HH} and ΔM_{HB} are parts of the dipolar second moments (amplitude) due to ^1H–^1H and ^1H–^{11}B interactions caused by the reorientational process. The parameters such as the activation energy E_a, pre-exponential factor τ_0, and amplitude ΔM were varied to obtain the best fit for the R_1^H data. The resulting fit is shown in by the red solid line in Fig. 4a. The corresponding fitting parameters are E_a = 0.35 ± 0.01 eV, τ_0 = 9 ± 0.05 × 10^{-16} s, $M_{H\text{-}H}$ = 4.5 ± 0.1 × 10^{10} s^{-2}, and $M_{H\text{-}B}$ = 2.10 ± 0.1 × 10^{10} s^{-2} respectively.

The ^{11}B relaxation rate R_1^B is ~2 orders of magnitude less than the Li relaxation rate, indicating that the quadrupolar interaction is the primary contributor to the relaxation mechanism. The contribution of the heteronuclear ^{11}B–^{1}H dipole-dipole interaction is negligible compared to that of the strong quadrupolar interaction. Therefore, the boron relaxation rate can be expressed using the following equation:

$$R_1^B = \frac{\omega_q^2}{50}\left[\frac{\tau_c}{1+\omega_B^2\tau_c^2} + \frac{4\tau_c}{1+4\omega_B^2\tau_c^2}\right]$$

The best fit is shown by the red solid line in Fig. 4a, where the best fit parameters are E_a = 0.38 eV, τ_0 = 3.25 ± 0.05 × 10^{-16} s, and ω_q^2 = 3.0 ± 0.1 × 10^{13} s^{-2}. Because the R_1^{Li}(T) maximum was observed at approximately the same temperature as R_1^H(T) and R_1^B(T), we can conclude that the cation jump rate was nearly equal to the anion reorientation rate within the region of the peaks.

The temperature-dependence of the correlation frequency τ^{-1} for 0.7Li(CB_9H_{10})–0.3Li($CB_{11}H_{12}$) extracted from the BPP fit is shown in Fig. S2. The correlation frequency for H, B, and Li was of the same order of magnitude (~10^9 s^{-1}) at ambient temperature (298 K). The correlation frequency of the order of ~10^9 s^{-1} for Li at ambient temperature confirms the fast translational motion of the cation, indicating that the conductivity is of the order of 0.1–1 mS cm^{-1} for ionic diffusion.[15] Moreover, the H jump frequency of 8.2 × 10^9 s^{-1} estimated from the NMR data for 0.7Li(CB_9H_{10})–0.3Li($CB_{11}H_{12}$) is in line with the H jump frequency (8.8 × 10^9 s^{-1}) for pristine Li(CB_9H_{10}) in the high-temperature disordered phase at 349 K.[16] The Li correlation (jump) rate τ_c (where a maximum was observed in the R_1^{Li} vs. $1/T$ plot) was found to be close to 0.6 ns at a temperature of 305 K. The jump rate derived from NMR relaxation measurements can be used to estimate the diffusion coefficient at a certain temperature using the Einstein [ES] equation.[34] The diffusion coefficient estimated using the ES equation is $D = a^2/6\tau$ = 7.67 × 10^{-12} m^2 s^{-1}, where the jump distance is assumed to be 1.5 Å assuming 3D-correlated diffusion. (see Fig. 4b). We previously measured the lithium diffusion coefficient using PFG-NMR (ms) and compared it with the diffusion coefficient calculated from the ionic conductivity (μs) using the Nernst-Einstein equation.[8] The diffusion coefficient calculated from the NMR relaxation rate matched well with that measured using PFG-NMR.[8] From these results, it is concluded that lithium-ion diffusion in 0.7Li(CB_9H_{10})–0.3Li($CB_{11}H_{12}$) occurs through the correlated motion of lithium ions over a wide timescale.

The activation energies for 0.7Li(CB_9H_{10})–0.3Li($CB_{11}H_{12}$), estimated for the cation and anion motion, were compared to those of the pristine compounds (Table 1). The activation energies for cation translational motion in pristine $LiCB_9H_{10}$ and $LiCB_{11}H_{12}$ (Table 1) are lower (<0.1 eV) than those of 0.7Li(CB_9H_{10})–0.3Li($CB_{11}H_{12}$) (0.35 eV). The temperature-dependent ^{7}Li NMR relaxation rate for $LiCB_9H_{10}$ reached a maximum at approximately 333 K, and a second relaxation process was observed above 360 K, which showed less temperature-dependence. Therefore, the lower activation energy for $LiCB_9H_{10}$ may be due to the estimation of the activation energy from the second process at temperatures higher than T_{max} (peak maximum temperature), which is less temperature-dependent (leading to a lower activation energy). Similar behavior was observed in $Na_2(B_{10}H_{10})_{0.5}$–$(B_{12}H_{12})_{0.5}$ with two relaxation processes. In the case of $Na_2(B_{10}H_{10})_{0.5}$–$(B_{12}H_{12})_{0.5}$, the second relaxation process at temperatures $>T_{max}$ is attributed to an additional slower diffusion process.[15] Furthermore, fitting the first relaxation peak for $Na_2(B_{10}H_{10})_{0.5}$–$(B_{12}H_{12})_{0.5}$ using a modified BPP model yielded an activation energy of 0.37 eV in the high-temperature region, consistent with the activation energy from the conductivity analysis. Similarly, using an appropriate model to fit the first relaxation peak for $LiCB_9H_{10}$ may result in a higher activation energy comparable to the activation energy estimated from the conductivity. These results suggest that sufficient care must be taken to accurately analyze the activation energy based on the relaxation rate.

The activation energies estimated for the anion reorientational motion in pristine $LiCB_9H_{10}$ (0.30 eV) and $LiCB_{11}H_{12}$ (0.40 eV) fell well within the line compared to those of 0.7Li(CB_9H_{10})–0.3Li($CB_{11}H_{12}$) (0.35 eV). Moreover, the activation energies for the anion reorientational motion (0.34 and 0.39 eV for R_1^H and R_1^B respectively) of 0.7Li(CB_9H_{10})–0.3Li($CB_{11}H_{12}$) (0.35 eV) matched well with that for the translational motion of the ^{7}Li cation. These results suggest that translational cation motion was coupled with anion reorientational motion. More importantly, the present investigations confirm that the activation energy for cation translational motion, estimated using the ^{7}Li NMR spin-lattice relaxation rate, ionic conductivity, and PFG-NMR, falls within the line (0.35 eV). The identical activation energies determine using different experimental techniques over a wide time-scale indicate that 0.7Li(CB_9H_{10})–0.3Li($CB_{11}H_{12}$) has a dynamically attenuated energy landscape through all sublattices of the cations over a wide range of time-scales. These unique phenomena are plausibly due to the highly disordered structures of both the cations and complex anions, enabling (random) cationic diffusion that is not dependent on the surrounding sublattice frameworks.[10,15]

Table 1. Activation energies in closoborate compounds determined using various techniques

Material	T_1				^{7}Li PFG-NMR		Cond	QENS	Ref
	^{1}H	^{11}B	^{7}Li	E_a (eV)	D (m^2/s)	E_a (eV)	E_a (eV)	E_a (eV)	
$Li_2B_{12}H_{12}$	○			1.4					9
$LiCB_9H_{10}$ (LT phase)	○			0.302					16
$LiCB_9H_{10}$ (HT phase)	○			0.299				0.17	16
$LiCB_9H_{10}$ (HT phase)			○	0.055			0.29		7
$LiCB_9H_{10}$					8×10^{-11} @363 K	0.265			20
$LiCB_{11}H_{12}$ (LT phase)	○			0.409					17
$LiCB_{11}H_{12}$ (LT phase)			○	0.422					17
$LiCB_{11}H_{12}$ (HT phase)	○			0.177					17
$LiCB_{11}H_{12}$ (HT phase)			○	0.092					17
$LiCB_{11}H_{12}$							0.22		24
$Li_2(CB_9H_{10})(CB_{11}H_{12})$	○			0.22					18
$0.7Li(CB_9H_{10})$–$0.3Li(CB_{11}H_{12})$					4.5×10^{-12} @298 K	0.35			8
$0.7Li(CB_9H_{10})$–$0.3Li(CB_{11}H_{12})$							0.37		8
$0.7Li(CB_9H_{10})$–$0.3Li(CB_{11}H_{12})$	○			0.35					This work
$0.7Li(CB_9H_{10})$–$0.3Li(CB_{11}H_{12})$		○		0.39					This work
$0.7Li(CB_9H_{10})$–$0.3Li(CB_{11}H_{12})$			○	0.35					This work

Finally, from the above discussion, it can be concluded that the ion dynamics in lithium-conducting solid electrolytes can be evaluated over a wide time-scale using NMR relaxation, AC impedance, and PFG-NMR measurement techniques. Although it is necessary to carefully choose suitable samples that show good structural stability and a flattened energy landscape, such samples were successfully developed herein by the partial replacement of closoborate anions in $LiCB_9H_{10}$.

The lithium-ion dynamics in the complex hydride $0.7Li(CB_9H_{10})$–$0.3Li(CB_{11}H_{12})$ were studied over a wide time-scale (ns–ms) using NMR relaxation, PFG-NMR, and AC impedance spectroscopy. The NMR relaxation rates of the cation (^7Li) and anion (^1H, ^{11}B) showed identical maxima with respect to temperature. Moreover, the activation energies estimated from the NMR relaxation rate measurements for the cation and anion are nearly the same (0.35 eV), clearly indicating that the Li-ion motion is highly correlated with the anion reorientational motion. Furthermore, the activation energies for Li ion motion estimated on different time-scales using AC impedance, ^7Li NMR relaxation, and ^7Li PFG-NMR were found to be nearly the same. The observation of similar activation energies over a wide time-scale indicates that the lithium-ion motion is homogeneous at all time-scales. The present measurements confirmed that the disordered phase obtained by mixing two closoborate anions resulted in an almost flat dynamic profile, leading to superionic lithium conduction. From a broader perspective, we suggest that understanding ion transport over a wide time-scale can provide useful insights into strategies for designing superionic conducting complex hydride materials.

Methods

The sample was prepared by a literature method.[8] The samples were transferred into 5 mm NMR tubes and sealed under argon atmosphere. ^7Li, ^{11}B, and ^1H NMR measurements were conducted using a JEOL ECA 300 NMR spectrometer at 116.6, 96.30, and 300.13 MHz respectively, using a special variable-temperature (213–423 K) wideband (^1H–^{15}N) NMR probe. The 1D NMR spectra were acquired using the standard 1-pulse pulse sequence with 1k acquisitions with a 90° pulse width of 12, 11, and 12 μs for ^7Li, ^{11}B, and ^1H nuclei respectively. Lithium chloride (1 M) in D_2O solution and 2 vol% tetramethylsilane (TMS) in $CDCl_3$ were used as external standards for referencing the ^7Li, and ^1H NMR chemical shifts (δ_{iso} = 0 ppm). Orthoboric acid (H_3BO_3) was used as an external reference for ^{11}B nuclei (δ_{iso} = 19.5 ppm). The anion and cation dynamics were studied using ^1H, ^{11}B, and ^7Li NMR spin-lattice relaxation time measurements over a wide temperature range (263–393 K). The ^7Li, ^{11}B, and ^1H spin-lattice relaxation times were measured using a conventional inversion recovery pulse sequence. Dry nitrogen gas was used to control the sample temperature, which was monitored using a Pt-Rh thermocouple. All NMR measurements were performed by decreasing the temperature. After reaching the desired temperature, a minimum waiting time of 15 min was used to ensure thermal equilibrium before starting the measurements.

ASSOCIATED CONTENT

Supporting Information

The following files are available free of charge.

Temperature dependence of the ^{1}H, ^{11}B NMR linewidth and correlation time (PDF)

AUTHOR INFORMATION

Notes

The authors declare no competing financial interests.

ACKNOWLEDGMENT

REFERENCES

(1) Inaguma, Y.; Liquan, C.; Itoh, M.; Nakamura, T.; Uchida, T.; Ikuta, H.; Wakihara, M, HIGH IONIC CONDUCTIVITY IN LITHIUM LANTHANUM TITANATE, *Solid State Commun.* **1993**, *86*, 689–693.

(2) Murugan, R.; Thangadurai, V.; Weppner, W, FAST LITHIUM ION CONDUCTION IN GARNET-TYPE $LI_7LA_3ZR_2O_{12}$. *Angew. Chem. Int. Ed. Engl.* **2007**, *46*, 7778–7781.

(3) Kamaya, N.; Homma, K.; Yamakawa, Y.; Hirayama, M.; Kanno, R.; Yonemura, M.; Kamiyama, T.; Kato, Y.; Hama, S.; Kawamoto, K.; Mitsui, A, A LITHIUM SUPERIONIC CONDUCTOR, *Nat. Mater.* **2011**, *10*, 682–686.

(4) Seino, Y.; Ota, T.; Takada, K.; Hayashi, A.; Tatsumisago, M, A SULPHIDE LITHIUM SUPER ION CONDUCTOR IS SUPERIOR TO LIQUID ION

CONDUCTORS FOR USE IN RECHARGEABLE BATTERIES, *Energy Environ. Sci.* **2014**, *7*, 627–631.

(5) Mohtadi, R.; Orimo, S.-I, THE RENAISSANCE OF HYDRIDES AS ENERGY MATERIALS, *Nat. Rev. Mater.* **2017**, *2*, 16091.

(6) Unemoto, A.; Ikeshoji, T.; Yasaku, Syun; Matsuo, M.; Stavila, V.; Udovic, T. J.; Orimo, S.-I, STABLE INTERFACE FORMATION BETWEEN TIS_2 AND $LIBH_4$ IN BULK-TYPE ALL-SOLID-STATE LITHIUM BATTERIES, *Chem. Mater.* **2015**, *27*, 5407–5416.

(7) Tang, W. S.; Matsuo, M.; Wu, H.; Stavila, V.; Zhou, W.; Talin, A. A.; Soloninin, A. V.; Skoryunov, R. V.; Babanova, O. A.; Skripov, A. V.; Unemoto, A.; Orimo, S.-I.; Udovic, T. J, LIQUID-LIKE IONIC CONDUCTION IN SOLID LITHIUM AND SODIUM MONOCARBA-CLOSO-DECABORATES NEAR OR AT ROOM TEMPERATURE, *Adv. Energy Mater.* **2016**, *6*, 1502237–1502240.

(8) Kim, Sangryun; Oguchi, H.; Toyama, N.; Sato, T.; Takagi, S.; Otomo, T.; Arunkumar, D.; Kuwata, N.; Kawamura, J.; Orimo, S. I, A COMPLEX HYDRIDE LITHIUM SUPERIONIC CONDUCTOR FOR HIGH-ENERGY-DENSITY ALL-SOLID-STATE LITHIUM METAL BATTERIES, *Nat. Commun.* **2019**, *10*, 1081.

(9) Verdal, N.; Her, J. H.; Stavila, V.; Soloninin, A. V.; Babanova, O. A.; Skripov, A. V.; Udovic, T. J.; Rush, J. J, COMPLEX HIGH-TEMPERATURE PHASE TRANSITIONS IN $LI_2B_{12}H_{12}$ AND $NA_2B_{12}H_{12}$, *J. Solid State Chem.* **2014**, *212*, 81–91.

(10) Kweon, K. E.; Varley, J. B.; Shea, P.; Adelstein, N.; Mehta, P.; Heo, T. W.; Udovic, T. J.; Stavila, V.; Wood, B. C, STRUCTURAL, CHEMICAL, AND DYNAMICAL FRUSTRATION: ORIGINS OF SUPERIONIC CONDUCTIVITY IN CLOSO-BORATE SOLID ELECTROLYTES, *Chem. Mater.* **2017**, *29*, 9142–9153.

(11) Verdal, N.; Udovic, T. J.; Stavila, V.; Tang, W. S.; Rush, J. J.; Skripov, A. V, ANION REORIENTATIONS IN THE SUPERIONIC CONDUCTING PHASE OF $NA_2B_{12}H_{12}$, *J. Phys. Chem. C* **2014**, *118*, 17483–17489.

(12) Skripov, A. V.; Babanova, O. A.; Soloninin, A. V.; Stavila, V.; Verdal, N.; Udovic, T. J.; Rush, J. J, NUCLEAR MAGNETIC RESONANCE STUDY OF ATOMIC MOTION IN $A_2B_{12}H_{12}$ (A = NA, K, RB, CS): ANION REORIENTATIONS AND NA^+ MOBILITY, *J. Phys. Chem. C* **2013**, *117*, 25961–25968.

(13) Martelli, P.; Remhof, A.; Borgschulte, A.; Ackermann, R.; Strässle, T.; Embs, J. P.; Ernst, M.; Matsuo, M.; Orimo, S.-I.; Züttel, A, ROTATIONAL MOTION IN $LIBH_4$/LII SOLID SOLUTIONS, *J. Phys. Chem. A* **2011**, *115*, 5329–5334.
(14) Klein, I. S.; Zhao, Z.-F.; Davidowski, S. K.; Yarger, J. L.; Angell, C. A, A NEW VERSION OF THE LITHIUM ION CONDUCTING PLASTIC CRYSTAL SOLID ELECTROLYTE, *Adv. Energy Mater.* New Version. **2018**, *8*, 1801324.
(15) Duchêne, L.; Lunghammer, S.; Burankova, T.; Liao, W.; Embs, J. P.; Copéret, C.; Wilkening, H. M. R.; Remhof, A.; Hagemann, H.; Battaglia, C, IONIC CONDUCTION MECHANISM IN THE $NA_2(B_{12}H_{12})_{0.5}(B_{10}H_{10})_{0.5}$ CLOSO-BORATE SOLID-STATE ELECTROLYTE: INTERPLAY OF DISORDER AND ION–ION INTERACTIONS, *Chem. Mater.* **2019**, *31*, 3449–3460.
(16) Soloninin, A. V.; Dimitrievska, M.; Skoryunov, R. V.; Babanova, O. A.; Skripov, A. V.; Tang, W. S.; Stavila, V.; Orimo, S. I.; Udovic, T. J, COMPARISON OF ANION REORIENTATIONAL DYNAMICS IN MCB_9H_{10} AND $M_2B_{10}H_{10}$ (M = LI, NA) VIA NUCLEAR MAGNETIC RESONANCE AND QUASIELASTIC NEUTRON SCATTERING STUDIES, *J. Phys. Chem. C*. **2017**, *121*, 1000–1012.
(17) Skripov, A. V.; Skoryunov, R. V.; Soloninin, A. V.; Babanova, O. A.; Tang, W. S.; Stavila, V.; Udovic, T. J, ANION REORIENTATIONS AND CATION DIFFUSION IN $LICB_{11}H_{12}$ AND $NACB_{11}H_{12}$:^{1}H, ^{7}LI, AND ^{23}NA NMR STUDIES, *J. Phys. Chem. C* **2015**, *119*, 26912–26918.
(18) Tang, W. S.; Yoshida, K.; Soloninin, A. V.; Skoryunov, R. V.; Babanova, O. A.; Skripov, A. V.; Dimitrievska, M.; Stavila, V.; Orimo, S.-I.; Udovic, T. J, STABILIZING SUPERIONIC-CONDUCTING STRUCTURES VIA MIXED-ANION SOLID SOLUTIONS OF MONOCARBA-CLOSO-BORATE SALTS, *ACS Energy Lett.* **2016**, *1*, 659–664.
(19) Soloninin, A. V.; Skoryunov, R. V.; Babanova, O. A.; Skripov, A. V.; Dimitrievska, M.; Udovic, T. J, COMPARISON OF ANION AND CATION DYNAMICS IN A CARBON-SUBSTITUTED CLOSO-HYDROBORATE SALT: ^{1}H AND ^{23}NA NMR STUDIES OF SOLID-SOLUTION $NA_2(CB_9H_{10})(CB_{11}H_{12})$, *J. Alloys Compd.* **2019**, *800*, 247–253.
(20) Skripov, A. V.; Majer, G.; Babanova, O. A.; Skoryunov, R. V.; Soloninin, A. V.; Ley, M. B.; Jensen, T. R.; Orimo, S.-I.; Udovic, T. J, LITHIUM-ION DIFFUSIVITY IN COMPLEX HYDRIDES: PULSED-FIELD-GRADIENT NMR STUDIES OF

$LiLa(BH_4)_3Cl$, $Li_3(NH_2)_2I$ AND $LiCB_9H_{10}$, *Solid State Ionics* **2021**, *362*, 115585–115591.

(21) Hayamizu, K.; Matsuda, Y.; Matsui, M.; Imanishi, N, LITHIUM ION DIFFUSION MEASUREMENTS ON A GARNET-TYPE SOLID CONDUCTOR $LI_{6.6}LA_3ZR_{1.6}TA_{0.4}O_{12}$ BY USING A PULSED-GRADIENT SPIN-ECHO NMR METHOD, *Solid State Nucl. Magn. Reson.* **2015**, *70*, 21–27.

(22) Dorai, A.; Kuwata, N.; Takekawa, R.; Kawamura, J.; Kataoka, K.; Akimoto, J, DIFFUSION COEFFICIENT OF LITHIUM IONS IN GARNET-TYPE $LI_{6.5}LA_3ZR_{1.5}TA_{0.5}O_{12}$ SINGLE CRYSTAL PROBED BY ^{7}LI PULSED FIELD GRADIENT-NMR SPECTROSCOPY, *Solid State Ionics* **2018**, *327*, 18–26.

(23) Hayamizu, K.; Seki, S.; Haishi, T, LITHIUM ION MICROMETER DIFFUSION IN A GARNET-TYPE CUBIC $LI_7LA_3ZR_2O_{12}$ (LLZO) STUDIED USING ^{7}LI NMR SPECTROSCOPY, *J. Chem. Phys.* **2017**, *146*, 024701.

(24) Tang, W. S.; Unemoto, A.; Zhou, W.; Stavila, V.; Matsuo, M.; Wu, H.; Orimo, S. I.; Udovic, T. J, UNPARALLELED LITHIUM AND SODIUM SUPERIONIC CONDUCTION IN SOLID ELECTROLYTES WITH LARGE MONOVALENT CAGE-LIKE ANIONS, *Energy Environ. Sci.* **2015**, *8*, 3637–3645.

(25) Heitjans, P.; Indris, S, DIFFUSION AND IONIC CONDUCTION IN NANOCRYSTALLINE CERAMICS, *J. Phys.: Condens. Matter*. **2003**, *15*, R1257–R1289.

(26) Sugiyama, J, ION DIffUSION IN SOLIDS PROBED BY MUON-SPIN SPECTROSCOPY, *J. Phys. Soc. Jpn.* **2013**, *82* Supplement A, SA023–SA033.

(27) David C. Ailion and William D. Ohlsen, SOLID STATE NUCLEAR METHODS:METHODS IN EXPERIMENTAL PHYSICS 21, -Academic Press, Massachusetts, USA, 1983.

(28) Epp, V.; Gün, Ö.; Deiseroth, H.-J.; Wilkening, M, HIGHLY MOBILE IONS: LOW-TEMPERATURE NMR DIRECTLY PROBES EXTREMELY FAST LI^+ HOPPING IN ARGYRODITE-TYPE LI_6PS_5BR, *J. Phys. Chem. Lett.* **2013**, *4*, 2118–2123.

(29) Abragam, A, THE PRINCIPLES OF NUCLEAR MAGNETISM, Clarendon Press: Oxford, UK, 1961.

(30) Richards, P. M, PHYSICS OF SUPERIONIC CONDUCTORS (TOPICS IN CURRENT PHYSICS, 15), Springer-Verlag, Berlin Heidelberg, 1979.

(31) Meyer, M.; Maass, P.; Bunde, A, SPIN-LATTICE RELAXATION: NON-BLOEMBERGEN-PURCELL-POUND BEHAVIOR BY STRUCTURAL DISORDER AND COULOMB INTERACTIONS, *Phys. Rev. Lett.* **1993**, *71*, 573–576.

(32) Kawamura, J.; Morota, K.; Kuwata, N.; Nakamura, Y.; Maekawa, H.; Hattori, T.; Imanaka, N.; Okazaki, Y.; Adachi, G.-Y, HIGH TEMPERATURE ^{31}P NMR STUDIES ON MG^{2+} ION CONDUCTORS, *Solid State Commun.* **2001**, *120*, 295–298.

(33) Berger, S.; Roos, J.; Zavidonov, A. Yu.; Brinkmann, D, ^{31}P NMR RELAXATION IN GLASSY 0.35LIF・$0.65LIPO_3$, Solid State Ionics **1998**, *112*, 87–93.

(34) Mehrer, H, DIFFUSION IN SOLIDS: FUNDAMENTALS, METHODS, MATERIALS, DIFFUSION-CONTROLLED PROCESSES, Springer-Verlag, Berlin, Heidelberg, 2007.